doi:10.1093/toxsci/kfs298
Advance Access publication November 7, 2012

Mechanisms of Hepatocellular Toxicity Associated with Dronedarone—A Comparison to Amiodarone

Andrea Felser,*,† Kim Blum,*,† Peter W. Lindinger,*,†,‡ Jamal Bouitbir,*,†,‡ and Stephan Krähenbühl*,†,‡,[1]

*Department of Clinical Pharmacology & Toxicology, University Hospital, 4031 Basel, Switzerland; and †Department of Biomedicine and ‡Swiss Center of Applied Human Toxicology (SCAHT), University of Basel, Basel, Switzerland

[1]To whom correspondence should be addressed. Fax: +41-61-265-4560. E-mail: kraehenbuehl@uhbs.ch.

Received September 4, 2012; accepted October 3, 2012

Dronedarone is a new antiarrhythmic drug with an amiodarone-like benzofuran structure. Shortly after its introduction, dronedarone became implicated in causing severe liver injury. Amiodarone is a well-known mitochondrial toxicant. The aim of our study was to investigate mechanisms of hepatotoxicity of dronedarone *in vitro* and to compare them with amiodarone. We used isolated rat liver mitochondria, primary human hepatocytes, and the human hepatoma cell line HepG2, which were exposed acutely or up to 24 h. After exposure of primary hepatocytes or HepG2 cells for 24 h, dronedarone and amiodarone caused cytotoxicity and apoptosis starting at 20 and 50 µM, respectively. The cellular ATP content started to decrease at 20 µM for both drugs, suggesting mitochondrial toxicity. Inhibition of the respiratory chain required concentrations of ~10 µM and was caused by an impairment of complexes I and II for both drugs. In parallel, mitochondrial accumulation of reactive oxygen species (ROS) was observed. In isolated rat liver mitochondria, acute treatment with dronedarone decreased the mitochondrial membrane potential, inhibited complex I, and uncoupled the respiratory chain. Furthermore, in acutely treated rat liver mitochondria and in HepG2 cells exposed for 24 h, dronedarone started to inhibit mitochondrial β-oxidation at 10 µM and amiodarone at 20 µM. Similar to amiodarone, dronedarone is an uncoupler and an inhibitor of the mitochondrial respiratory chain and of β-oxidation both acutely and after exposure for 24 h. Inhibition of mitochondrial function leads to accumulation of ROS and fatty acids, eventually leading to apoptosis and/or necrosis of hepatocytes. Mitochondrial toxicity may be an explanation for hepatotoxicity of dronedarone *in vivo*.

Key Words: **benzofuran derivatives; mitochondria; uncoupling; electron transport chain; apoptosis.**

Amiodarone is a well-established antiarrhythmic drug (Julian *et al*., 1997; Morse *et al*., 1988), which is associated with several potentially severe adverse reactions (Mason, 1987; Stelfox *et al*., 2004). Importantly, it is a hepatic mitochondrial toxicant (Lewis *et al*., 1989, 1990; Morse *et al*., 1988), which has been described to uncouple oxidative phosphorylation, to inhibit enzyme complexes of the electron transport chain and to impair fatty acid β-oxidation (Fromenty *et al*., 1990; Fromenty and Pessayre, 1995; Kaufmann *et al*., 2005; Spaniol *et al*., 2001; Waldhauser *et al*., 2006). Mitochondrial β-oxidation and oxidative phosphorylation are fundamental physiological processes as evidenced by inherited impairment of these pathways, which can affect the function of many organs, including the liver (Krahenbuhl *et al*., 1999). Patients treated with amiodarone for several months or years may thus suffer from micro- and/or macrovesicular steatosis, a disease that may progress to steatohepatitis and may eventually be fatal (Lewis *et al*., 1990; Simon *et al*., 1984).

Dronedarone, a structural analog of amiodarone, was specifically designed to minimize the adverse reactions associated with amiodarone (Dobrev and Nattel, 2010). As shown in Figure 1, dronedarone is a noniodinated amiodarone derivative carrying a methylsulfonamide group at the benzofurane ring that decreases its lipophilicity. Similar to amiodarone, dronedarone is metabolized by N-desalkylation of the basic side chain by cytochrome P450 (CYP) 3A4 (Patel *et al*., 2009). Although the N-desalkylated metabolites are toxic for amiodarone (Waldhauser *et al*., 2006; Zahno *et al*., 2011), this is currently not known for dronedarone.

Shortly after its introduction, severe hepatic injury has been reported in two patients treated with dronedarone, eventually leading to liver transplantation (Anonymous, 2011). Recently, Serviddio *et al.* (2011) published a study in which they investigated liver mitochondrial toxicity of dronedarone and amiodarone *in vivo* in rats. Similar to previous studies (Fromenty *et al*., 1990; Kaufmann *et al*., 2005; Spaniol *et al*., 2001), amiodarone inhibited the activity of complex I of the respiratory chain, uncoupled oxidative phosphorylation, and was associated with increased reactive oxygen species (ROS) production and lipid peroxidation. In contrast, dronedarone only uncoupled oxidative phosphorylation, but was not associated with inhibition of the respiratory chain or increased ROS production.

In this study, we aimed to investigate and to better understand the mechanisms of cytotoxicity of dronedarone *in vitro* using isolated rat liver mitochondria, primary human hepatocytes,

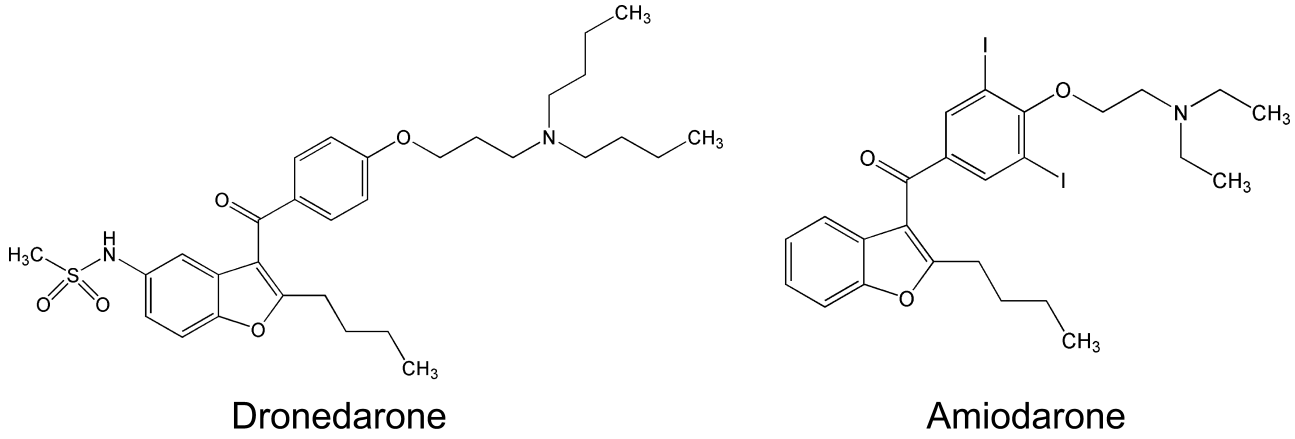

FIG. 1. Chemical structures of dronedarone and amiodarone.

and HepG2 cells, a well-characterized human hepatoma cell line (Zahno *et al*., 2011). We compared the toxic effects associated with dronedarone with those of amiodarone. Because the two drugs are structurally related (Fig. 1) and both can cause hepatic injury, we hypothesized that their mechanism of toxicity may be similar. The systems used allowed to study the toxicity acutely and after different exposure periods as well as after cytochrome P450 (CYP) induction.

MATERIALS AND METHODS

Chemicals. Dronedarone hydrochloride was extracted from commercially available tablets (brand name Multaq) from ReseaChem life science GmbH (Burgdorf, Switzerland). The manufacturer declared the substance 99% pure by high-performance liquid chromatography and confirmed the structure by ^{1}H-NMR analysis. Amiodarone hydrochloride was purchased from Sigma-Aldrich (Buchs, Switzerland). Stock solutions were prepared in dimethylsulfoxide (DMSO) and stored at −20°C. All other chemicals used were purchased from Sigma-Aldrich or Fluka, except where indicated.

Cell lines and cell culture. The human hepatoma cell line HepG2 was provided by ATCC (Manassas, VA) and maintained in Dulbecco's Modified Eagle Medium (DMEM, with 1.0 g/l glucose, 4mM L-glutamine, and 1mM pyruvate) from Invitrogen (Basel, Switzerland). The culture medium was supplemented with 10% (vol/vol) heat-inactivated fetal calf serum, 2mM GlutaMax, 10mM 4-(2-hydroxyethyl)-1-piperazineethanesulfonic acid (HEPES) buffer and nonessential amino acids. Cell culture supplements were all purchased from GIBCO (Paisley, UK). Cells were kept at 37°C in a humidified 5% CO_2 cell culture incubator and were passaged using trypsin. The cell number was determined using a Neubauer hemacytometer and viability using the trypan blue exclusion method.

Cryopreserved primary human hepatocytes were purchased from Becton Dickinson (BD Gentest, Woburn, MA). They were recovered and cultured according to the protocol of the manufacturer. Induction of CYP3A4 was achieved by preincubation of recovered primary human hepatocytes with 20µM rifampicin for 72 h (Zahno *et al*., 2011).

Rat liver mitochondria. Male Sprague Dawley rats were kept in the animal facility of the University Hospital Basel (Basel, Switzerland) in a temperature-controlled environment with a 12-h light/dark cycle and food and water *ad libitum*. Animal procedures were conducted in accordance with the institutional guidelines for the care and use of laboratory animals. The mean rat weight was 433 ± 79 g and the mean liver weight 12 ± 4 g. Rats were sacrificed by pentobarbital overdose (100 mg/rat), and liver mitochondria were isolated by differential centrifugation according to the method of Hoppel *et al.* (1979). The mitochondrial protein content was determined using the bicinchoninic acid (BCA) protein assay kit from Merck (Darmstadt, Germany).

Cytotoxicity. Cytotoxicity was determined using ToxiLight BioAssay Kit (Lonza, Basel, Switzerland) according to the manufacturer's manual. This assay measures the release of adenylate kinase, a marker for loss of cell membrane integrity, using a firefly luciferase system. After drug incubation, 100 µl assay buffer was added to 20µl supernatant from drug-treated cell culture medium, and luminescence was measured after incubation in the dark for 5 min, using a Tecan M200 Pro Infinity plate reader (Männedorf, Switzerland).

Intracellular ATP content. Intracellular ATP was determined using CellTiterGlo Luminescent cell viability assay (Lonza), in accordance with the manufacturer's manual. In brief, 100 µl assay buffer was added to each 96-well containing 100 µl culture medium. After incubation in the dark for 30 min, luminescence was measured using a Tecan M200 Pro Infinity plate reader.

Annexin V and propidium iodide staining. Apoptosis and necrosis were investigated using annexin V and propidium iodide (PI) staining (Invitrogen). Cells were treated with the test compounds for 24 h and stained with 1 µl annexin V-Alexa Fluor 647 and 1 µl propidium iodide 100 µg/ml in 100 µl annexin V binding buffer (10mM HEPES, 140mM NaCl, 2.5mM $CaCl_2$ in H_2O, pH 7.4). Cells were incubated for 15 min at room temperature (RT) and analyzed by flow cytometry using a CyAn ADP cytometer (Beckman Coulter, Marseille, France). Data were analyzed using FlowJo 9.3.2 software (Tree Star, Ashland, OR).

Caspase 3/7 assay. Caspase 3/7 activity was determined using the luminescent Caspase-Glo 3/7 Assay (Promega, Wallisellen, Switzerland). The assay was conducted according to the manufacturer's protocol.

Cytochrome c release. Quantitative determination of cytochrome c was performed as described by Waterhouse and Trapani (2003). HepG2 cells (100,000) were harvested and permeabilized with digitonin (10 µg/ml in Dulbecco's PBS [DPBS] without calcium) at RT for 20 min. Cells were fixed in paraformaldehyde (4% in DPBS) for 20 min at RT and were washed with blocking buffer (bovine serum albumin [BSA] 10% in DPBS) for 1 h and incubated over night at 4°C with 1:1000 purified mouse anti-cytochrome c monoclonal antibody (BD Pharmingen, Basel, Switzerland) in blocking buffer. Cells were washed with blocking buffer and incubated for 1 h with 1:1000 Alexa Fluor 488-labeled secondary antibody (Alexa Fluor 488 goat anti-mouse IgG, Invitrogen). After an additional washing step with DPBS, the cell suspensions were examined by flow cytometry. Because the selective permeabilization of the plasma membrane allows cytoplasmic cytochrome c to diffuse out of the

cell, mitochondrial release of cytochrome c into the cytoplasm leads to a low cellular cytochrome c content.

Cellular oxygen consumption using the Seahorse XF24 analyzer. Cellular respiration was measured using a Seahorse XF24 analyzer (Seahorse Biosciences, North Billerica, MA). HepG2 cells were seeded in Seahorse XF 24-well culture plates at 20,000 cells/well in DMEM growth medium and allowed to adhere overnight. Cells were treated with the drugs for 24 h. Before the experiment, the medium was replaced with 750 µl unbuffered medium using an XF Prep Station (Seahorse Biosciences), and cells were equilibrated for 40 min at 37°C in a CO_2-free incubator. Basal oxygen consumption was determined in the presence of glutamate/pyruvate (4 and 1mM, respectively). After inhibition of mitochondrial phosphorylation by adding oligomycin (1µM) to determine the oxidative leak, the mitochondrial electron transport chain was stimulated maximally by the addition of the uncoupler carbonyl cyanide *p*-(trifluoromethoxyl)-phenyl-hydrozone (FCCP, 1µM). Finally, the extramitochondrial respiration was determined after the addition of the complex I inhibitor rotenone (1µM). For the determination of the basal respiration, the oxidative leak, and maximal respiration, extramitochondrial respiration was subtracted.

Respiration by permeabilized HepG2 cells and isolated mitochondria. The activity of specific enzyme complexes of the respiratory chain was analyzed using an Oxygraph-2k high-resolution respirometer equipped with DatLab software (Oroboros Instruments, Innsbruck, Austria). Freshly isolated rat liver mitochondria or HepG2 cells were suspended in MiR06 (mitochondrial respiration medium containing 0.5mM EGTA, 3mM $MgCl_2$, 60mM K-lactobionate, 20mM taurine, 10mM KH_2PO_4, 20mM HEPES, 110mM sucrose, 1 g/l fatty acid-free BSA, and 280 U/ml catalase, pH 7.1) and transferred to the precalibrated oxygraph chambers.

Activities of complexes I and II were assessed in isolated rat liver mitochondria using L-glutamate/malate (10 and 2mM, respectively) as substrates, followed by the addition of ADP (2.5mM) and succinate/rotenone (10mM and 0.5µM, respectively). The oxidative leak, a measure for uncoupling, was determined by assessing the residual oxygen consumption after addition of oligomycin (1µM). Uncoupling was achieved by the addition of FCCP (1µM).

The activities of complexes I, II, III, and IV were assessed in HepG2 cells permeabilized with digitonin (10 µg/1 million cells). In a first run, complexes I and III were analyzed using L-glutamate/malate as substrate followed by the addition of ADP and the inhibitor rotenone. Afterwards, duroquinol (500µM, Tokyo Chemical Industry, Tokyo, Japan) was added to investigate complex III and inhibited with antimycin A (2.5µM). In a second run, complexes II and IV were analyzed using succinate/rotenone as substrate, followed by the addition of ADP and the inhibitor antimycin A. Afterwards N,N,N´,N´-tetramethyl-p-phenylenediamine/ascorbate (0.5 and 2mM, respectively) was added to investigate complex IV and inhibited with KCN (1mM).

We confirmed the integrity of the outer mitochondrial membrane by showing the absence of a stimulatory effect of exogenous cytochrome c (10µM) on respiration. Respiration was expressed as oxygen consumption per mg protein. Protein concentrations were determined using the Pierce BCA protein assay kit from Merck.

Mitochondrial membrane potential. The mitochondrial membrane potential was determined as described by Kaufmann *et al.* (2005) with some modifications. Freshly isolated rat liver mitochondria were washed with incubation buffer containing 137mM sodium chloride, 4.74mM potassium chloride, 2.56mM calcium chloride, 1.18mM potassium phosphate, 1.18mM magnesium chloride, 10mM HEPES, and 1 g/l glucose (pH 7.4). Then, mitochondria were incubated at 37°C in incubation buffer containing 0.5 µl/ml [phenyl-^{3}H]-tetraphenylphosphonium bromide (40 Ci/mmol, Anawa trading SA, Wangen, Switzerland). After 15 min, the suspension was centrifuged and the mitochondrial pellet resuspended in fresh nonradioactive incubation buffer. Afterwards, mitochondria were treated with test substances for 1 h at 37°C and centrifuged. After the incubation, radioactivity of the mitochondrial pellet was measured on a Packard 1900 TR liquid scintillation analyzer.

Mitochondrial accumulation of reactive oxygen species. HepG2 cells were stained with Hoechst 33342 trihydrochloride trihydrate (final concentration 20 µg/ml DMEM, Invitrogen) for 30 min at 37°C, followed by the addition of and MitoSOX red (final concentration 5µM in DMEM, Invitrogen) and dronedarone (5, 10, and 20µM) or amiodarone (10, 20, and 50µM). Real-time accumulation of superoxide was analyzed over 6 h using a Cellomics ArrayScan VTI HCS Reader (Thermo scientific, Pittsburg, PA).

mRNA expression of superoxide dismutase 1 and superoxide dismutase 2. The mRNA expression of superoxide dismutase 1 (SOD1) and superoxide dismutase 2 (SOD2) was assessed using real-time PCR as described previously (Mullen *et al*., 2011). HepG2 cells were treated for 24 h, and RNA was extracted and purified using the Qiagen RNeasy mini extraction kit (Qiagen, Hombrechtikon, Switzerland). The purity and quantity of RNA were evaluated with the NanoDrop 2000 (Thermo Scientific, Wohlen, Switzerland), and cDNA was synthesized from 10 µg RNA using the Qiagen omniscript system. The real-time PCR was performed in triplicate using SYBR Green (Roche Diagnostics, Rotkreuz, Basel). We used primers specific for the cytosolic SOD1 (forward: 5´-TGGCCGATGTGTCTATTGAA-3´, reverse: 5´-ACCTTTGCCCAAGTCATCTG-3´) and mitochondrial SOD2 (forward: 5´-GGTTGTTCACGTAGGCCG-3´,reverse:5´-CAGCAGGCAGCTGGCT-3´) and calculated relative quantities of specifically amplified cDNA with the comparative-threshold cycle method. GAPDH was used as endogenous reference (forward: 5´-CATGGCCTTCCGTGTTCCTA-3´; reverse: 5´-CCTGCTTCACCACCTTCTTGA-3´) and no-template and no-reverse-transcription controls were used to exclude nonspecific amplification (Mullen *et al*., 2011).

Mitochondrial β-oxidation. Metabolism of [1-^{14}C] palmitic acid (60 mCi/mmol; PerkinElmer, Schwerzenbach, Switzerland) was assessed via the formation of ^{14}C-acid–soluble β-oxidation products. Experiments were performed as previously described (Kaufmann *et al*., 2005) with some modifications. Isolated rat liver mitochondria were incubated for 15 min in the presence of the test compounds in assay buffer (200µM Na-palmitate, 0.1 pCi/ml [1-^{14}C] palmitic acid (60 mCi/mmol), 70mM sucrose, 43mM KCl, 3.6mM $MgCl_2$, 7.2mM KH_2PO_4, 36mM Tris, 2mM ATP, 500µM L-carnitine, 150µM coenzyme A, 50mM acetoacetate, 170µM BSA essentially fatty acid free, pH 7.4) at 37°C in a thermomixer at 600 rpm (Eppendorf, Switzerland). HepG2 cells were permeabilized with digitonin (10 µg/million cells) after drug exposure for 24 h and incubated for 1 h in the same assay buffer. The reactions were stopped by adding 400 µl 20% perchloric acid, and samples were precipitated for 20 min on ice before centrifugation (10,000 × g, 2 min). Radioactivity was measured in the supernatant.

Intracellular lipid accumulation. Experiments were performed as described by Donato *et al.* (2009). HepG2 cells were exposed for 24 h to exogenous lipids (DMEM containing 62µM of a 2:1 mixture of oleate and palmitate). Cells were treated with toxicants in lipid-free medium for 24 h, and intracellular lipid accumulation was measured using BODIPY 493/503 (final concentration 3.75 ng/ml), a nonpolar derivative of the BODIPY fluorophore (Donato *et al*., 2009). Cell suspensions were stained for 30 min at 37°C in Hank's buffered salt solution buffer in the dark, before examining by flow cytometry without any additional washing step. In order to exclude nonviable cells, PI was added and the analysis was restricted to live-cell populations.

Statistical methods. Data are given as the mean ± SEM of at least three independent experiments. Statistical analyses were performed using GraphPad Prism 5 (GraphPad Software, La Jolla, CA). One-way ANOVA was used for comparisons of more than two groups, followed by the comparisons between incubations containing toxicants and the control group using Dunnett's posttest procedure. Differences between induction experiments were compared using two-way ANOVA followed by Bonferroni's *post hoc* test. *P*-values < 0.05 (*) or < 0.01 (**) were considered significant.

RESULTS

Cytotoxicity in Primary Human Hepatocytes and HepG2 Cells

In primary human hepatocytes, dronedarone caused adenylate kinase release starting at a concentration of 20µM after treatment for 6 or 24 h, whereas amiodarone was not toxic up to 100µM

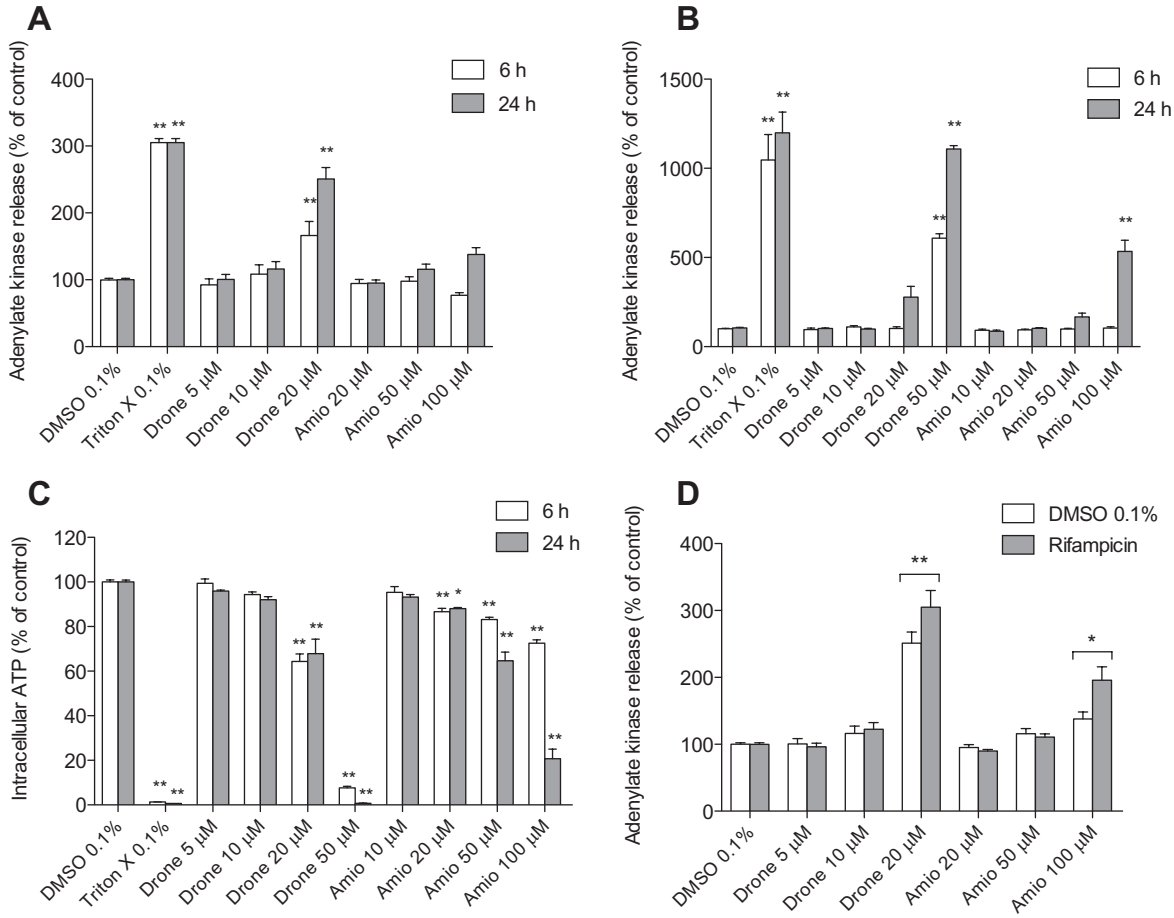

FIG. 2. Cytotoxicity and effect on intracellular ATP content. Cytotoxicity was assessed using the Toxi-Light assay. (A) Cytotoxicity in primary human hepatocytes after drug exposure for 6 or 24 h. (B) Cytotoxicity in HepG2 cells after drug exposure for 6 or 24 h. (C) Intracellular ATP content in HepG2 cells expressed as a percentage of the values obtained for DMSO (control). (D) Effect of pretreatment with rifampicin on cytotoxicity. Primary human hepatocytes were pretreated with rifampicin and then exposed to dronedarone or amiodarone for 24 h. CYP induction by rifampicin was associated with a 21% increase in cytotoxicity for dronedarone and a 42% increase for amiodarone. If not indicated otherwise, cytotoxicity data are expressed as percent increase compared with DMSO control. Drone: dronedarone, Amio: amiodarone. Data represent the mean ± SEM of at least three independent experiments. $*p < 0.05$ versus DMSO control. $**p < 0.01$ versus DMSO control.

(Fig. 2A). In HepG2 cells, dronedarone and amiodarone were both toxic starting at 50 and 100µM, respectively (Fig. 2B). Intracellular ATP started to decrease at 20µM for both dronedarone and amiodarone after exposure for 6 or 24 h, suggesting that mitochondria were affected before cytotoxicity could be demonstrated (Fig. 2C). CYP3A4 induction by rifampicin increased the cytotoxicity of both 100µM amiodarone (42%) and 20µM dronedarone (21%). Considering the only small increase in dronedarone-associated cytotoxicity with CYP3A4 induction, the following studies were carried out with the parent compounds only.

Acute Effects on Isolated Rat Liver Mitochondria

Reduced cellular ATP content was compatible with impaired mitochondrial function, which has been reported previously for amiodarone (Fromenty *et al.*, 1990; Spaniol *et al.*, 2001; Waldhauser *et al.*, 2006). As shown in Figure 3A, both amiodarone and dronedarone reduced the membrane potential of isolated rat liver mitochondria, confirming this assumption. Both toxicants impaired concentration dependently the maximal function of the electron transport chain in the presence of oligomycin and FCCP and acted as uncouplers of oxidative phosphorylation as evidenced by an increase of the respiratory leak in the presence of oligomycin (Figs. 3B and 3C). Further investigation of oxidative phosphorylation revealed a concentration-dependent decrease of state 3 respiration in the presence of L-glutamate/malate by both toxicants (Figs. 4A and 4B). With succinate as substrate, the inhibition was less pronounced, showing only for amiodarone a significant inhibition of state 3 respiration at 50µM (Figs. 4A and 4B).

Subacute Mitochondrial Toxicity in HepG2 Cells

The oxygen consumption of intact HepG2 cells was assessed at drug concentrations that were not cytotoxic in previous

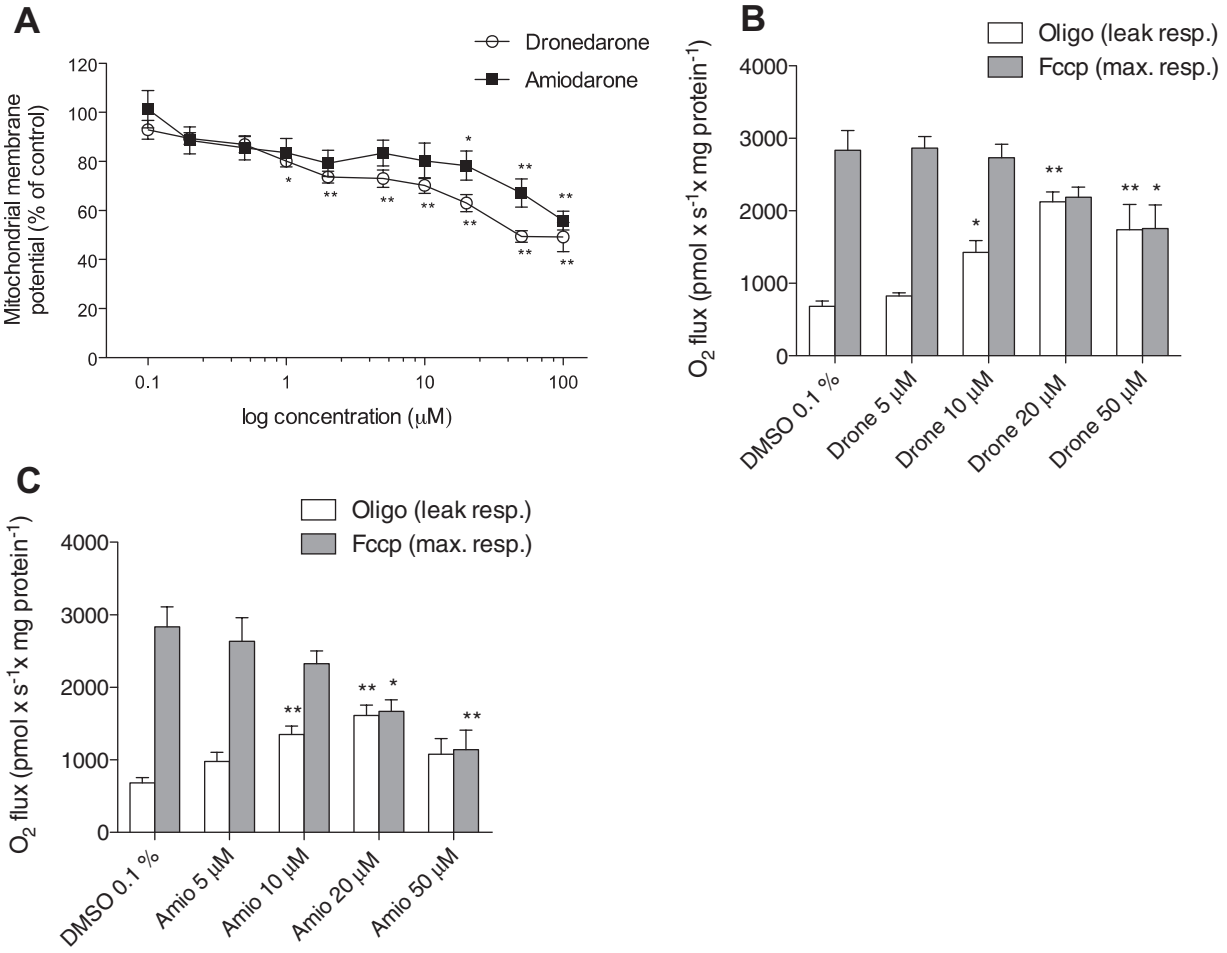

FIG. 3. Effect on membrane potential and oxidative metabolism of freshly isolated rat liver mitochondria. (A) Mitochondria were labeled with [^{3}H]-tetraphenylphosphonium bromide, and mitochondrial accumulation of radioactivity was determined. DMSO served as control and was set at 100%. (B) and (C) Acute effect of dronedarone and amiodarone on the respiratory leak (respiration in the presence of oligomycin) and maximal (FCCP-induced) respiration after acute drug exposure. Drone: dronedarone, Amio: amiodarone, Oligo: oligomycin. Data represent the mean ± SEM of at least three individual preparations. *$p < 0.05$ versus control. **$p < 0.01$ versus control.

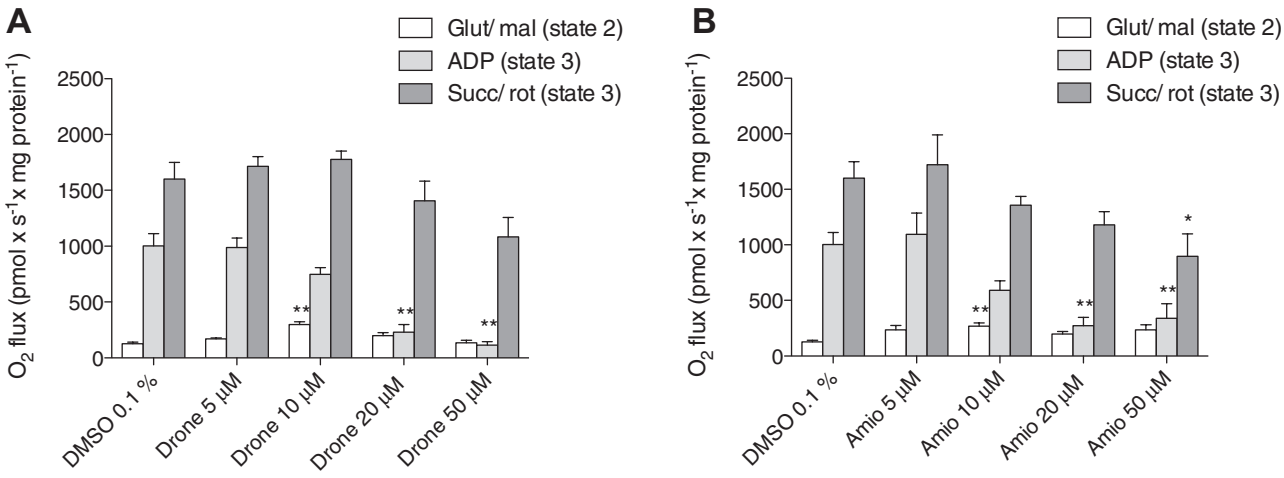

FIG. 4. Acute effect of dronedarone and amiodarone on oxidative metabolism of freshly isolated rat liver mitochondria. Glut/mal: glutamate/malate, Succ/rot: succinate/rotenone, Drone: dronedarone, Amio: amiodarone. Data represent the mean ± SEM. *$p < 0.05$ versus control. **$p < 0.01$ versus control.

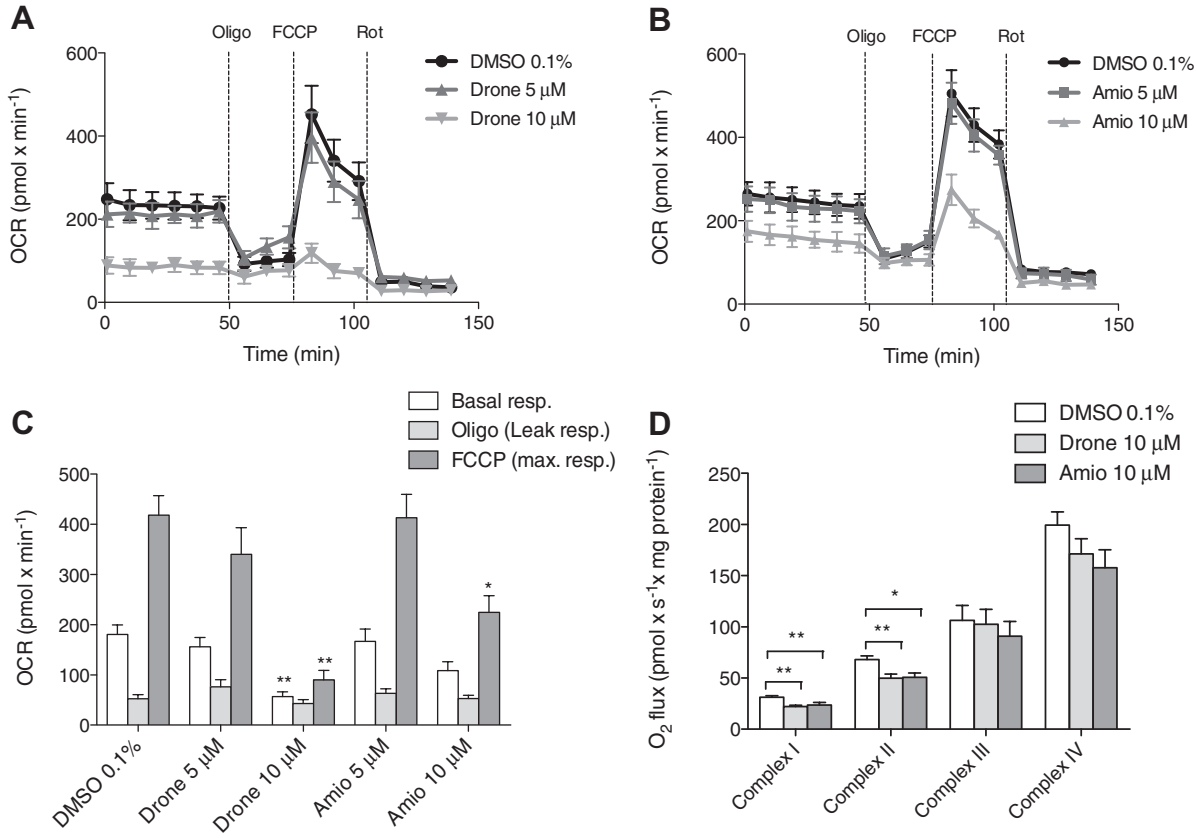

FIG. 5. Subacute effect of dronedarone and amiodarone on oxidative metabolism of HepG2 cells. (A) and (B) Oxygen consumption rate after 24 h exposure for dronedarone or amiodarone measured on the Seahorse XF24 analyzer. (C) Basal respiration, oxidative leak, and maximal respiration after 24 h drug exposure measured on the Seahorse XF24 analyzer. (D) Respiratory capacity through complexes I, II, III, and IV after 24 h drug exposure measured on the Oxygraph-2k high-resolution respirometer. Drone: dronedarone, Amio: amiodarone, Oligo: oligomycin. Data present the mean ± SEM. $*p < 0.05$, $**p < 0.01$ versus control.

experiments. Figures 5A and 5B show oxygen consumption of HepG2 cells after treatment with vehicle (DMSO), dronedarone (5µM, 10µM), or amiodarone (5µM, 10µM) for 24 h. A concentration of 5µM did not significantly decrease basal and maximal respiration for both drugs, whereas the higher concentration decreased maximal (uncoupled) respiration for both drugs significantly (Fig. 5C). The respiratory leak after the addition of oligomycin was not significantly increased by the toxicants (Fig. 5C), suggesting that dronedarone and amiodarone had no uncoupling effect in HepG2 cells exposed for 24 h at these low concentrations.

In order to investigate the mechanism of decreased maximal respiration, the respiratory capacities through the complexes of the electron transport chain were analyzed using high-resolution respirometry. After exposure to 10µM dronedarone or amiodarone for 24 h, the respiratory capacities through complexes I and II were decreased for both drugs (Fig. 5D).

As expected from toxicants inhibiting complex I (Drose and Brandt, 2012), mitochondrial superoxide accumulated in HepG2 cells when exposed to the toxicants (Figs. 6A and 6B). At the same time, mRNA expression of mitochondrial SOD2 was increased, whereas the expression of the cytoplasmic SOD1 remained unchanged (Fig. 6C), underscoring that dronedarone and amiodarone mainly affect mitochondria.

Effect on Mitochondrial β-Oxidation and Cellular Accumulation of Fatty Acids

Mitochondrial β-oxidation was monitored by the formation of acid-soluble β-oxidation products from palmitate in isolated rat liver mitochondria after acute exposure to dronedarone and amiodarone. Dronedarone started to inhibit β-oxidation by isolated rat liver mitochondria at 20µM and amiodarone at 100µM (Fig. 7A). In permeabilized HepG2 cells after 24 h drug exposure, dronedarone started to inhibit mitochondrial β-oxidation at 10µM and amiodarone at 20µM (Fig. 7B). As a consequence, intracellular lipid accumulation was significant after exposure to 20µM dronedarone or 50µM amiodarone for 24 h.

Mechanisms of Cell Death in HepG2 Cells

In order to investigate the mechanism of cell death, externalization of phosphatidylserine was analyzed using annexin V and disintegration of cell membranes with PI. Flow cytometric analysis of HepG2 cells revealed a progressive increase of

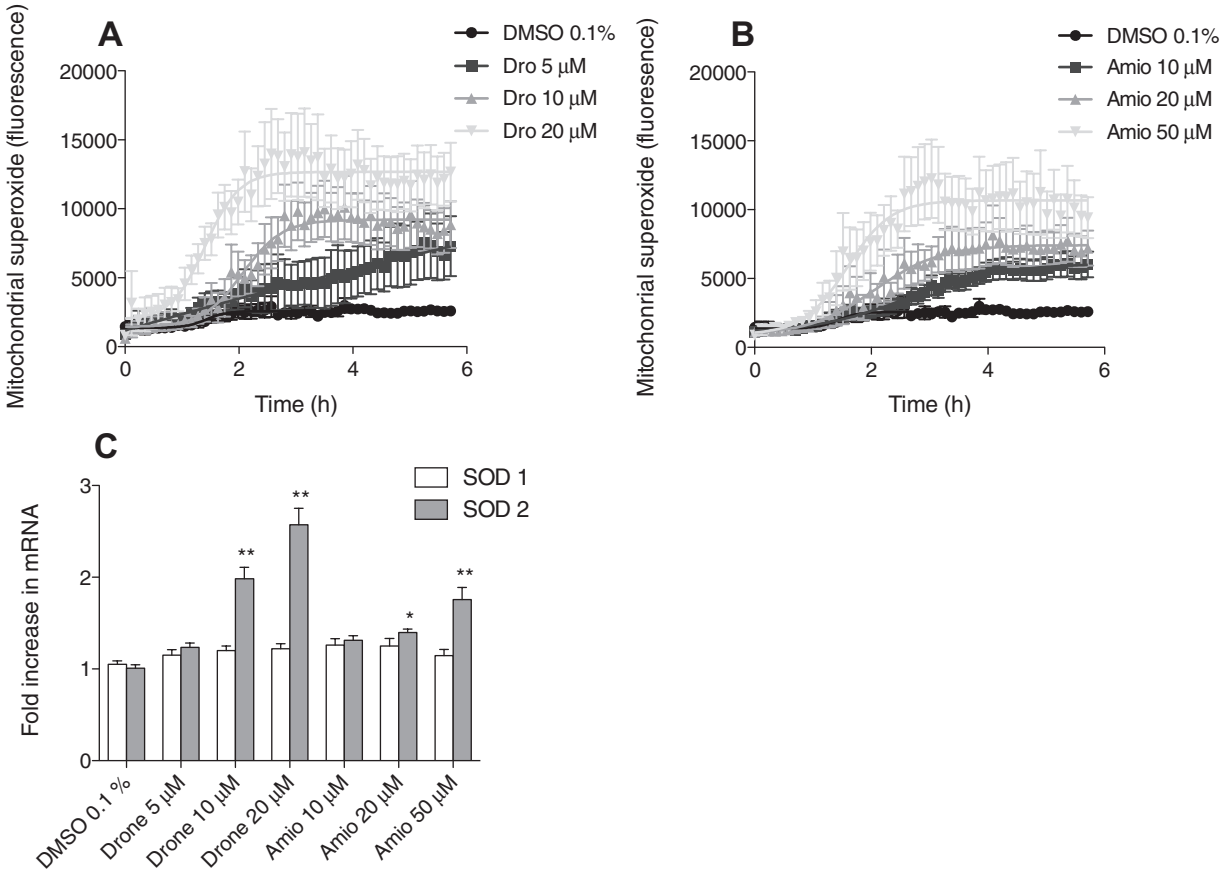

FIG. 6. Mitochondrial ROS production and SOD expression by HepG2 cells. (A) and (B) Mitochondrial ROS accumulation in the presence of dronedarone or amiodarone for 24 h. (C) mRNA expression of SOD1, SOD2 in HepG2 cells after exposure to dronedarone or amiodarone for 24 h. Drone: dronedarone, Amio: amiodarone. Data present the mean ± SEM. $*p < 0.05$, $**p < 0.01$ versus control.

early and late apoptotic cells with increasing concentrations of dronedarone or amiodarone (Fig. 8A). The activity of caspases 3/7, key mediators of apoptosis, was increased after treatment with 20µM dronedarone for 6 or 24 h, and after treatment with 50µM amiodarone for 24 h (Fig. 8B). Furthermore, the release of cytochrome c from mitochondria was significant after 6 or 24 h of incubation with 5µM dronedarone and with 20µM or 5µM amiodarone, respectively (Fig. 8C). Mitochondrial release of cytochrome c is a marker of permeabilization of the mitochondrial outer membrane, activating the intrinsic apoptotic pathway (Antico Arciuch *et al*., 2012).

DISCUSSION

Our investigations demonstrate that both dronedarone and amiodarone are uncouplers and inhibitors of the mitochondrial respiratory chain and also inhibit mitochondrial β-oxidation. Furthermore, exposure to dronedarone and amiodarone was associated with cellular superoxide accumulation and lipid storage, eventually leading to apoptosis and/or necrosis.

Both compounds tested were toxic for isolated liver mitochondria, primary human hepatocytes, and HepG2 cells. They impaired mitochondrial function starting at concentrations between 10 and 20µM, whereas cytotoxicity was observed at higher concentrations, namely 20µM for dronedarone and 50µM for amiodarone. At therapeutic dosages, amiodarone reaches plasma concentrations in the range of ~2µM (Lafuente-Lafuente *et al*., 2009). In liver, amiodarone concentrations are 10–20 times higher than in plasma (Wyss *et al*., 1990), suggesting that the results of this study are clinically relevant. This assumption is supported by the observation that in 104 patients treated with amiodarone and followed prospectively, 25 developed an increase in serum transaminases and 3 out of these 25 patients symptomatic liver injury (Lewis *et al*., 1989). For dronedarone, plasma concentrations reached at therapeutic dosages are in the range of 0.2µM (Patel *et al*., 2009), which is ~50 times lower than the lowest concentration where we started to observe mitochondrial toxicity. Dronedarone is almost completely absorbed and its bioavailability is only 15% (Hoy and Keam, 2009), suggesting that the hepatic concentrations may be higher than in plasma. This may even more so in patients

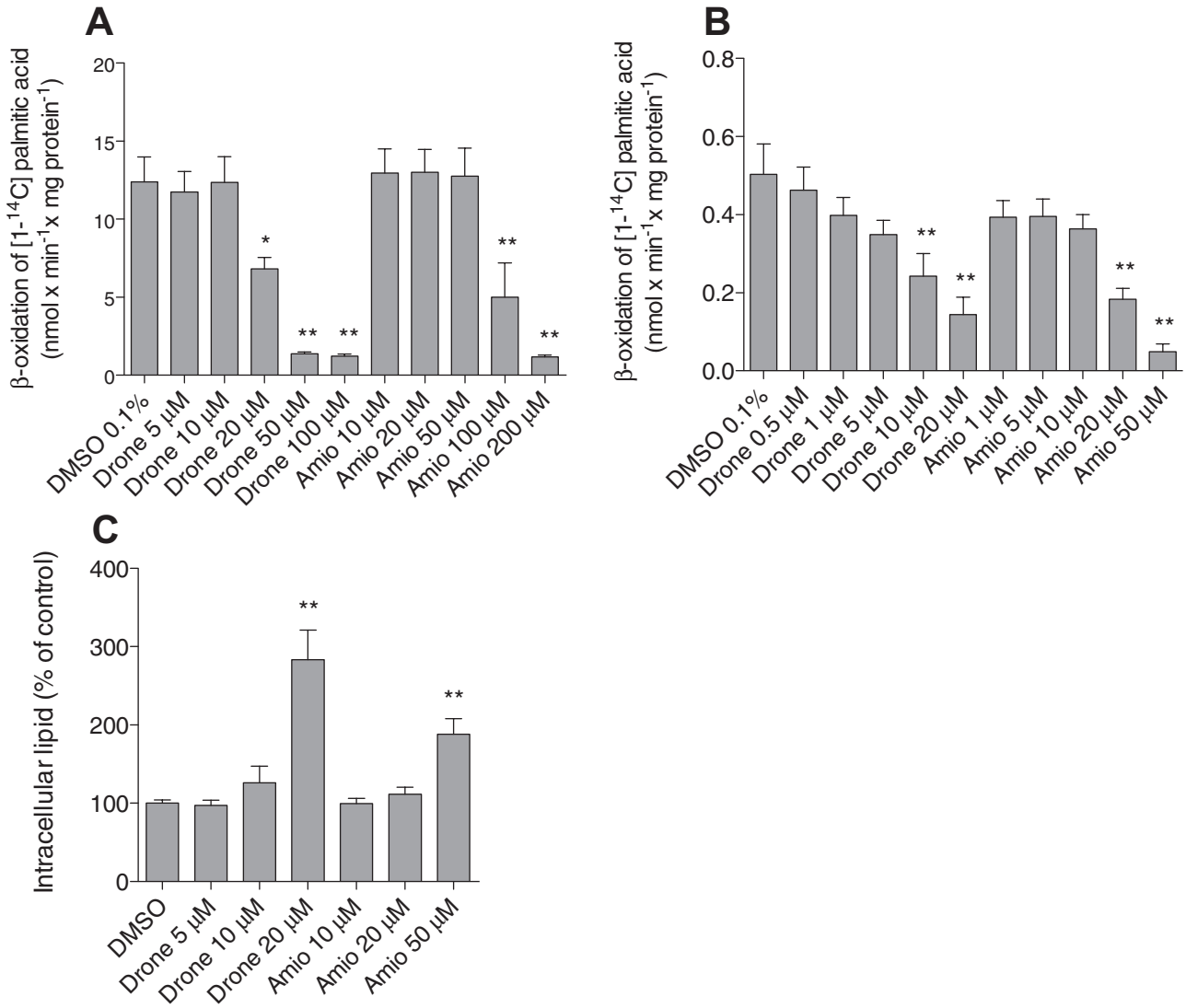

FIG. 7. Effect on mitochondrial β-oxidation and intracellular fat accumulation. (A) Freshly isolated rat liver mitochondria were exposed to test compounds and acute inhibition of the rate of β-oxidation was determined. (B) HepG2 cells were exposed to test compounds for 24 h and β-oxidation was determined in permeabilized cells. (C) Intracellular triglyceride accumulation in HepG2 cells after drug exposure for 24 h. Drone: dronedarone, Amio: amiodarone. Data present the mean ± SEM. *$p < 0.05$ versus control. **$p < 0.01$ versus control.

with low hepatic CYP3A4 activity, in particular in patients treated concomitantly with CYP3A4 inhibitors, because dronedarone is metabolized mainly by CYP3A4 (Dorian, 2010; Patel *et al*., 2009). Although dronedarone was at least as toxic as amiodarone in this study, slightly less patients appear to develop liver injury during treatment with dronedarone compared with amiodarone. In large clinical studies, between 0.6 and 13.6% of the patients treated with dronedarone have been reported to develop liver injury (Connolly *et al*., 2011; Hohnloser *et al*., 2009; Singh *et al*., 2007). The large variation can be explained by different definitions of liver injury and by the patients included into the studies. No patient in these studies developed symptomatic liver injury. The apparently lower hepatic toxicity of dronedarone compared with amiodarone in clinical studies may at least partially be explained by the assumption that the tissue accumulation of dronedarone is less accentuated than for amiodarone due to the lower lipophilicity of dronedarone (Hoy and Keam, 2009). As a consequence, as discussed above, only specific patients may reach high enough hepatic concentrations which lead to hepatocyte damage.

Our data suggest that the toxicity of dronedarone is mainly caused by the parent compound. In comparison to amiodarone, the N-dealkylated metabolites appear to play a less important role for the toxicity (Fig. 2D). The question concerning the toxicity of the N-dealkylated metabolites is clinically important, because, as we have shown in an *in vitro* study for amiodarone, CYP3A4 induction is a risk factor for hepatotoxicity, because the N-dealkylated metabolites are even more hepatotoxic than

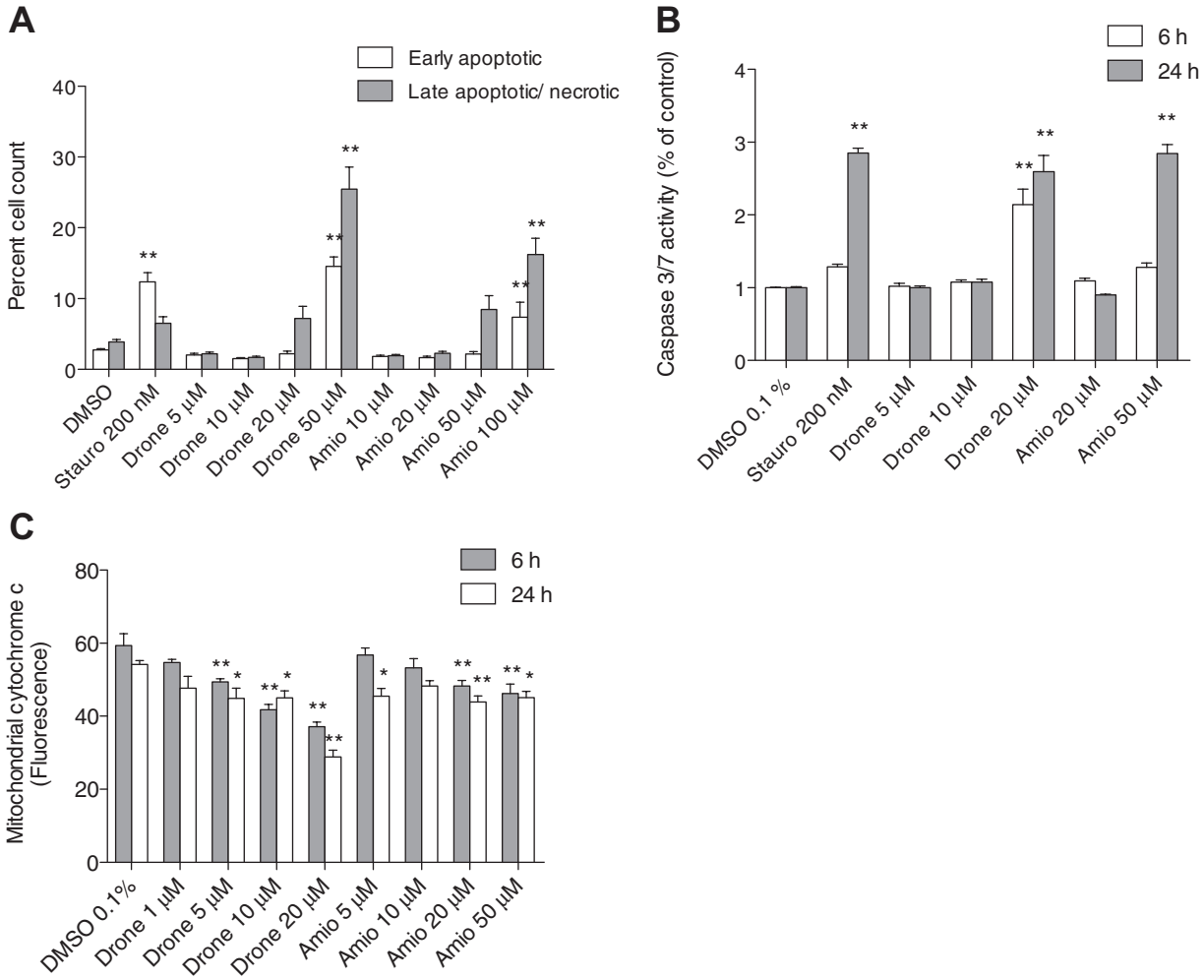

FIG. 8. Mechanisms of cell death. (A) Annexin V binding and PI uptake by HepG2 cells which were exposed for 24 h to test compounds. The samples were analyzed using flow cytometry. Early apoptotic populations are stained only with annexin V and late apoptotic represent annexin V and PI double-stained populations, undergoing necrosis or later stages of apoptosis. Staurosporine was used as a positive control for apoptosis. Data are presented as percent cell count. (B) Caspase 3/7 activity after drug exposure for 6 and 24 h, expressed as percent increase compared with DMSO control. (C) Mitochondrial cytochrome c content after drug exposure for 6 and 24 h expressed as fluorescence intensity measured by flow cytometry. Stauro: staurosporine, Drone: dronedarone, Amio; amiodarone. Data represent the mean ± SEM of at least three independent experiments. $*p < 0.05$ versus DMSO control $**p < 0.01$ versus DMSO control.

amiodarone (Waldhauser *et al*., 2006; Zahno *et al*., 2011). For dronedarone, this question can only be answered accurately, however, when toxicological studies can be carried out with the corresponding N-dealkylated metabolites.

The toxicity of dronedarone and amiodarone on the electron transport chain was quite similar. Both drugs inhibited complex I and uncoupled oxidative phosphorylation in isolated liver mitochondria in a concentration-dependent manner. Amiodarone inhibited also complex II, a finding observed for dronedarone only in HepG2 cells, but not in isolated rat liver mitochondria. For amiodarone, such findings have already been described in previous studies (Fromenty *et al*., 1990; Spaniol *et al*., 2001; Waldhauser *et al*., 2006). For dronedarone, they are not surprising, taking into account its structure with a benzofurane ring carrying a butyl side chain. These structural properties have been described in a previous study from our laboratory as being sufficient for mitochondrial toxicity (Kaufmann *et al*., 2005). Importantly, the effects of both drugs on mitochondrial respiration were observed at lower concentrations than those required for cytotoxicity; taking into account the concentration dependency, it is likely that mitochondrial toxicity is a major reason for the cytotoxicity of these compounds. In contrast to our study, Serviddio *et al.* (2011) had not observed an inhibition of enzyme complexes of the electron transport chain in liver mitochondria isolated from rats treated with dronedarone. This discrepancy with our study may be explained by the observation that small molecules such as drugs can diffuse out of the mitochondria during the isolation procedure (Spaniol *et al*., 2003). In our experiments, we used either isolated mitochondria which were exposed to a known drug concentration

or permeabilized hepatocytes, in which the local environment of the mitochondria should not have changed much during the experimental procedures. Alternatively, the exposure in the study of Serviddio *et al.* (2011), may have been lower than in our *in vitro* investigations. In their study, Serviddio *et al*. used a dosage of ~40 mg dronedarone per kg body weight and they did not determine serum or tissue concentrations.

Besides affecting the electron transport chain, dronedarone and amiodarone also efficiently inhibited mitochondrial β-oxidation. Steatosis during the treatment with amiodarone is well established (Lewis *et al*., 1990; Simon *et al*., 1984) and may be a result from impaired β-oxidation (Fromenty and Pessayre, 1995; Kaufmann *et al*., 2005). A likely mechanism how amiodarone inhibits β-oxidation is by inhibiting carnitine palmitoyltransferase 1 (Kennedy *et al*., 1996), which is considered to be rate limiting for β-oxidation. In contrast to amiodarone, the effects of dronedarone on the individual steps of β-oxidation are currently not known. The inhibition of mitochondrial β-oxidation has several consequences. As shown in the current and in previous investigations (Begriche *et al*., 2011; Spaniol *et al*., 2003), free fatty acids, acyl-CoAs, and triglycerides accumulate and may be toxic in hepatocytes. Accumulating free fatty acids have been described to uncouple oxidative phosphorylation, to increase ROS production, and to induce mitochondrial permeability transition, eventually leading to apoptosis (Rial *et al*., 2010).

Both inhibition of the electron transport chain (especially complexes I and/or III) (Drose and Brandt, 2012; Liu *et al*., 2002) and inhibition of β-oxidation (Kaufmann *et al*., 2005) are associated with increased mitochondrial production of ROS. In the presence of inhibitors of complex I or III, electrons may escape from the electron transport chain and react with molecular oxygen to form superoxide (Liu *et al*., 2002). Under normal conditions, superoxide is degraded by intramitochondrial antioxidative systems such as glutathione peroxidase and superoxide dismutase (Bouitbir *et al*., 2012; Troy and Shelanski, 1994). The observed increase of the mRNA expression of mitochondrial SOD2 after treatment with 20μM dronedarone or 50μM amiodarone can therefore be regarded as a compensatory mechanism to counteract increased mitochondrial ROS production. The lacking increase of cytosolic SOD1 mRNA expression suggests that ROS production was primarily intramitochondrial. An increase of mitochondrial ROS production is a trigger for opening of the mitochondrial membrane permeability transition pore, which is associated with cytochrome c release into the cytoplasm and induction of apoptosis and/or necrosis (Antico Arciuch *et al*., 2012). Mitochondrial release of cytochrome c and apoptosis could clearly be demonstrated in our study.

In conclusion, our investigations demonstrate that dronedarone inhibits the electron transport chain and β-oxidation and uncouples oxidative phosphorylation of liver mitochondria. Inhibition of complex I and of β-oxidation is associated with increased mitochondrial ROS production, which triggers mitochondrial membrane permeability transition and apoptosis. These findings may explain liver toxicity observed in predisposed patients.

FUNDING

Swiss National Science Foundation (SNF 31003A-132992 to S.K.).

REFERENCES

Anonymous. (2011). In brief: FDA warning on dronedarone (Multaq). *Med. Lett. Drugs Ther.* **53,** 17.

Antico Arciuch, V. G., Elguero, M. E., Poderoso, J. J., and Carreras, M. C. (2012). Mitochondrial regulation of cell cycle and proliferation. *Antioxid. Redox Signal.* **16,** 1150–1180.

Begriche, K., Massart, J., Robin, M. A., Borgne-Sanchez, A., and Fromenty, B. (2011). Drug-induced toxicity on mitochondria and lipid metabolism: Mechanistic diversity and deleterious consequences for the liver. *J. Hepatol.* **54,** 773–794.

Bouitbir, J., Charles, A. L., Echaniz-Laguna, A., Kindo, M., Daussin, F., Auwerx, J., Piquard, F., Geny, B., and Zoll, J. (2012). Opposite effects of statins on mitochondria of cardiac and skeletal muscles: A 'mitohormesis' mechanism involving reactive oxygen species and PGC-1. *Eur. Heart J.* **33,** 1397–1407.

Connolly, S. J., Camm, A. J., Halperin, J. L., Joyner, C., Alings, M., Amerena, J., Atar, D., Avezum, Á., Blomström, P., Borggrefe, M., *et al.* (2011). Dronedarone in high-risk permanent atrial fibrillation. *N. Engl. J. Med.* **365,** 2268–2276.

Dobrev, D., and Nattel, S. (2010). New antiarrhythmic drugs for treatment of atrial fibrillation. *Lancet*. **375,** 1212–1223.

Donato, M. T., Martínez-Romero, A., Jiménez, N., Negro, A., Herrera, G., Castell, J. V., O'Connor, J. E., and Gómez-Lechón, M. J. (2009). Cytometric analysis for drug-induced steatosis in HepG2 cells. *Chem. Biol. Interact.* **181,** 417–423.

Dorian, P. (2010). Clinical pharmacology of dronedarone: Implications for the therapy of atrial fibrillation. *J. Cardiovasc. Pharmacol. Ther.* **15**(4 Suppl.), 15S–18S.

Drose, S., and Brandt, U. (2012). Molecular mechanisms of superoxide production by the mitochondrial respiratory chain. *Adv. Exp. Med. Biol.* **748,** 145–169.

Fromenty, B., Fisch, C., Berson, A., Letteron, P., Larrey, D., and Pessayre, D. (1990). Dual effect of amiodarone on mitochondrial respiration. Initial protonophoric uncoupling effect followed by inhibition of the respiratory chain at the levels of complex I and complex II. *J. Pharmacol. Exp. Ther.* **255,** 1377–1384.

Fromenty, B., and Pessayre, D. (1995). Inhibition of mitochondrial beta-oxidation as a mechanism of hepatotoxicity. *Pharmacol. Ther.* **67,** 101–154.

Hohnloser, S. H., Crijns, H. J., van Eickels, M., Gaudin, C., Page, R. L., Torp-Pedersen, C., and Connolly, S. J. (2009). Effect of dronedarone on cardiovascular events in atrial fibrillation. *N. Engl. J. Med.* **360,** 668–678.

Hoppel, C., DiMarco, J. P., and Tandler, B. (1979). Riboflavin and rat hepatic cell structure and function. Mitochondrial oxidative metabolism in deficiency states. *J. Biol. Chem.* **254,** 4164–4170.

Hoy, S. M., and Keam, S. J. (2009). Dronedarone. *Drugs* **69,** 1647–1663.

Julian, D. G., Camm, A. J., Frangin, G., Janse, M. J., Munoz, A., Schwartz, P. J., and Simon, P. (1997). Randomised trial of effect of amiodarone on mortality in patients with left-ventricular dysfunction after recent myocardial infarction: EMIAT. European Myocardial Infarct Amiodarone Trial Investigators. *Lancet* **349,** 667–674.

Kaufmann, P., Török, M., Hänni, A., Roberts, P., Gasser, R., and Krähenbühl, S. (2005). Mechanisms of benzarone and benzbromarone-induced hepatic toxicity. *Hepatology* **41,** 925–935.

Kennedy, J. A., Unger, S. A., and Horowitz, J. D. (1996). Inhibition of carnitine palmitoyltransferase-1 in rat heart and liver by perhexiline and amiodarone. *Biochem. Pharmacol.* **52,** 273–280.

Krahenbuhl, S., Kleinle, S., Henz, S., Leibundgut, K., Liechti, S., Zimmermann, A., and Wiesmann, U. (1999). Microvesicular steatosis, hemosiderosis and rapid development of liver cirrhosis in a patient with Pearson's syndrome. *J. Hepatol.* **31,** 550–555.

Lafuente-Lafuente, C., Alvarez, J. C., Leenhardt, A., Mouly, S., Extramiana, F., Caulin, C., Funck-Brentano, C., and Bergmann, J. F. (2009). Amiodarone concentrations in plasma and fat tissue during chronic treatment and related toxicity. *Br. J. Clin. Pharmacol.* **67,** 511–519.

Lewis, J. H., Mullick, F., Ishak, K. G., Ranard, R. C., Ragsdale, B., Perse, R. M., Rusnock, E. J., Wolke, A., Benjamin, S. B., and Seeff, L. B. (1990). Histopathologic analysis of suspected amiodarone hepatotoxicity. *Hum. Pathol.* **21,** 59–67.

Lewis, J. H., Ranard, R. C., Caruso, A., Jackson, L. K., Mullick, F., Ishak, K. G., Seeff, L. B., and Zimmerman, H. J. (1989). Amiodarone hepatotoxicity: Prevalence and clinicopathologic correlations among 104 patients. *Hepatology* **9,** 679–685.

Liu, Y., Fiskum, G., and Schubert, D. (2002). Generation of reactive oxygen species by the mitochondrial electron transport chain. *J. Neurochem.* **80,** 780–787.

Mason, J. W. (1987). Amiodarone. *N. Engl. J. Med.* **316,** 455–466.

Morse, R. M., Valenzuela, G. A., Greenwald, T. P., Eulie, P. J., Wesley, R. C., and McCallum, R. W. (1988). Amiodarone-induced liver toxicity. *Ann. Intern. Med.* **109,** 838–840.

Mullen, P. J., Zahno, A., Lindinger, P., Maseneni, S., Felser, A., Krähenbühl, S., and Brecht, K. (2011). Susceptibility to simvastatin-induced toxicity is partly determined by mitochondrial respiration and phosphorylation state of Akt. *Biochim. Biophys. Acta* **1813,** 2079–2087.

Patel, C., Yan, G. X., and Kowey, P. R. (2009). Dronedarone. *Circulation* **120,** 636–644.

Rial, E., Rodríguez-Sánchez, L., Gallardo-Vara, E., Zaragoza, P., Moyano, E., and González-Barroso, M. M. (2010). Lipotoxicity, fatty acid uncoupling and mitochondrial carrier function. *Biochim. Biophys. Acta* **1797,** 800–806.

Serviddio, G., Bellanti, F., Giudetti, A. M., Gnoni, G. V., Capitanio, N., Tamborra, R., Romano, A. D., Quinto, M., Blonda, M., Vendemiale, G., *et al.* (2011). Mitochondrial oxidative stress and respiratory chain dysfunction account for liver toxicity during amiodarone but not dronedarone administration. *Free Radic. Biol. Med.* **51,** 2234–2242.

Simon, J. B., Manley, P. N., Brien, J. F., and Armstrong, P. W. (1984). Amiodarone hepatotoxicity simulating alcoholic liver disease. *N. Engl. J. Med.* **311,** 167–172.

Singh, B. N., Connolly, S. J., Crijns, H. J., Roy, D., Kowey, P. R., Capucci, A., Radzik, D., Aliot, E. M., and Hohnloser, S. H. (2007). Dronedarone for maintenance of sinus rhythm in atrial fibrillation or flutter. *N. Engl. J. Med.* **357,** 987–999.

Spaniol, M., Bracher, R., Ha, H. R., Follath, F., and Krähenbühl, S. (2001). Toxicity of amiodarone and amiodarone analogues on isolated rat liver mitochondria. *J. Hepatol.* **35,** 628–636.

Spaniol, M., Kaufmann, P., Beier, K., Wüthrich, J., Török, M., Scharnagl, H., März, W., and Krähenbühl, S. (2003). Mechanisms of liver steatosis in rats with systemic carnitine deficiency due to treatment with trimethylhydraziniumpropionate. *J. Lipid Res.* **44,** 144–153.

Stelfox, H. T., Ahmed, S. B., Fiskio, J., and Bates, D. W. (2004). Monitoring amiodarone's toxicities: Recommendations, evidence, and clinical practice. *Clin. Pharmacol. Ther.* **75,** 110–122.

Troy, C. M., and Shelanski, M. L. (1994). Down-regulation of copper/zinc superoxide dismutase causes apoptotic death in PC12 neuronal cells. *Proc. Natl. Acad. Sci. U.S.A.* **91,** 6384–6387.

Waldhauser, K. M., Török, M., Ha, H. R., Thomet, U., Konrad, D., Brecht, K., Follath, F., and Krähenbühl, S. (2006). Hepatocellular toxicity and pharmacological effect of amiodarone and amiodarone derivatives. *J. Pharmacol. Exp. Ther.* **319,** 1413–1423.

Waterhouse, N. J., and Trapani, J. A. (2003). A new quantitative assay for cytochrome c release in apoptotic cells. *Cell Death Differ.* **10,** 853–855.

Wyss, P. A., Moor, M. J., and Bickel, M. H. (1990). Single-dose kinetics of tissue distribution, excretion and metabolism of amiodarone in rats. *J. Pharmacol. Exp. Ther.* **254,** 502–507.

Zahno, A., Brecht, K., Morand, R., Maseneni, S., Török, M., Lindinger, P. W., and Krähenbühl, S. (2011). The role of CYP3A4 in amiodarone-associated toxicity on HepG2 cells. *Biochem. Pharmacol.* **81,** 432–441.